Annals of Hepatology 29 (2024) 101536

Contents lists available at ScienceDirect

Annals of Hepatology

journal homepage: www.elsevier.es/annalsofhepatology

Original article

CircROBO1 knockdown improves the radiosensitivity of hepatocellular carcinoma by regulating RAD21

Kai Yang[a,1], Yanpeng Ding[a,1], Jun Han[b,*], Rui He[a,*]

[a] Department of Oncology, Xiangyang Central Hospital, Affiliated Hospital of Hubei University of Arts and Science, Xiangyang City, 441000, Hubei, PR China
[b] Department of Interventional Radiology, Xiangyang Central Hospital, Affiliated Hospital of Hubei University of Arts and Science, Xiangyang City, 441000, Hubei, PR China

ARTICLE INFO

Article History:
Received 16 October 2023
Accepted 22 March 2024
Available online 14 August 2024

Keywords:
Hepatocellular carcinoma
CircROBO1
miR-136−5p
RAD21

ABSTRACT

Introduction and Objectives: Radioresistance is a common problem in the treatment of many cancers, including hepatocellular carcinoma (HCC). Previous studies have shown that circROBO1 is highly expressed in HCC tissues and acts as a cancer promoter to accelerate the malignant progression of HCC. However, the role and mechanism of circROBO1 in HCC radioresistance remain unclear.

Materials and Methods: CircROBO1, microRNA (miR)-136-5p and RAD21 expression levels were analyzed by quantitative real-time PCR. Cell function and radioresistance were evaluated by colony formation assay, cell counting kit 8 assay, EdU assay and flow cytometry. Protein expression was determined using western blot analysis. RNA interaction was analyzed by dual-luciferase reporter assay and RNA pull-down assay. In vivo experiments were performed by constructing mice xenograft models.

Results: CircROBO1 was highly expressed in HCC, and its knockdown inhibited HCC cell proliferation and promoted apoptosis to enhance cell radiosensitivity. On the mechanism, circROBO1 could serve as miR-136-5p sponge to positively regulate RAD21. MiR-136-5p inhibitor or RAD21 overexpression reversed the regulation of circROBO1 knockdown on the radiosensitivity of HCC cells. Also, circROBO1 interference improved the radiosensitivity of HCC tumors in vivo.

Conclusions: CircROBO1 might be a promising target for treating HCC radioresistance.

© 2024 Fundación Clínica Médica Sur, A.C. Published by Elsevier España, S.L.U. This is an open access article under the CC BY-NC-ND license (http://creativecommons.org/licenses/by-nc-nd/4.0/)

1. Introduction

Hepatocellular carcinoma (HCC) is a common pathological type of primary liver cancer, with high morbidity and mortality [1,2]. Although HCC treatment has made great progress, it is still a major challenge to effectively prolong the overall survival rate of patients [3,4]. Clinically, irradiation (IR) therapy is one of the main treatments for HCC, but the occurrence of IR resistance is still an important obstacle to HCC treatment [5,6]. Therefore, the discovery of new radiosensitization targets is necessary for the development of effective HCC treatment strategies.

With the continuous development of the RNA field, the importance of circular RNA (circRNA) in human diseases has received increasing attention from researchers [7,8]. Recently, many circRNAs are involved in cancer malignant progression and associated with cancer radioresistance [9]. For example, circ_0000554 was considered to be a tumor promoter in esophageal cancer, which enhanced cell growth and radioresistence by acting as miR-485−5p sponge to upregulate FERMT1 level [10]. Also, a recently research indicated that circABCB10 regulated the miR-223−3p/PFN2 axis to accelerate the proliferation and radioresistence of breast cancer [11]. In hepatoma-related studies, knockdown of circZNF292 had been discovered to suppress hepatoma radioresistance under hypoxia condition by inhibiting Wnt/β-catenin pathway [12]. Combined with previous findings, we believe that circRNA is a potential key target for treating the radioresistance of HCC.

In view of the potential of circRNA as a radiosensitization target for HCC, we focused on exploring new circRNAs that regulated the radioresistance of HCC. By analyzing the differentially expressed circRNA in GEO database, we found a significantly overexpressed circRNA, circ_0066568 (derived from ROBO1 gene, also called circROBO1), in HCC tissues. Meng *et al.* suggested that circROBO1 was highly expressed in HCC tissues and acted as a cancer promoter to accelerate the malignant progression of HCC [13]. However, whether circROBO1 regulates the radioresistance process of HCC remains

Abbreviations: HCC, hepatocellular carcinoma; IR, irradiation; circRNA, circular RNA; WB, western blot; IHC, immunohistochemistry; qRT-PCR, quantitative real-time PCR; CCK8, cell counting kit 8; miRNA, microRNA; OD, optical density; PS, phosphatidylserine; PI, propidium Iodide

* Corresponding authors.
E-mail addresses: hanjun0126@126.com (J. Han), 363161014@qq.com (R. He).

[1] These authors contributed equally to this paper.

https://doi.org/10.1016/j.aohep.2024.101536
1665-2681/© 2024 Fundación Clínica Médica Sur, A.C. Published by Elsevier España, S.L.U. This is an open access article under the CC BY-NC-ND license (http://creativecommons.org/licenses/by-nc-nd/4.0/)

unclear. Through detection, we discovered that circROBO1 expression in the tumor tissues of IR-resistant HCC patients was higher than that in IR-sensitive patients. Therefore, we speculated that circROBO1 might be related to radioresistance of HCC. According to this hypothesis, we carried out functional tests to verify the function of circROBO1 and further revealed the underlying molecular mechanism.

2. Materials and methods

2.1. Samples collection

HCC tumor tissues and matched adjacent normal tissues were obtained from 75 HCC patients (35 IR-sensitive and 40 IR-resistant) at Xiangyang Central Hospital, Affiliated Hospital of Hubei University of Arts and Science. Inclusion criteria: aged <70 years old, with HCC confirmed by histopathology; had received radiotherapy for the first time; exhibited normal heart, liver and kidney function. Exclusion criteria: patients with other cancers or a history of treatment for other cancers. The clinicopathologic features of 75 patients with HCC were listed in Table 1. All the specimens were stored at −80 °C.

2.2. Cell culture and treatment

The selection of cells was based on previous studies [14,15]. Human liver epithelial cells (THLE-2) and HCC cells (MHCC97H: high malignancy grade, HBV-positive and have high levels of stem-like lateral population cells; Huh7: low malignancy grade, HBV-negative and capable of producing some cytoplasmic proteins) (Biovector NTCC, Beijing, China) were cultured in BEGM Bullet Kit (Lonza, Walkersville, MD, USA) and DMEM medium containing 10% FBS (Gibco, Waltham, MA, USA). The circROBO1 lentiviral short hairpin RNA (sh-circROBO1), miR-136-5p mimic and inhibitor (in-miR-136-5p), pcDNA RAD21 overexpression vector (pcDNA-RAD21), and their controls (Genepharma, Shanghai, China) were transfected into HCC cells with Lipofectamine 3000 (Invitrogen, Carlsbad, CA, USA). For IR treatment, the transfected cells were exposed to 4 Gy X-ray radiation for 48 h. All cells were tested to confirm the absence of Mycoplasma contamination by using the MycoBlue Mycoplasma Detector (Vazyme, Nanjing, China).

Table 1
Association between clinicopathologic features and circROBO1 expression in 75 patients with HCC.

Features	circROBO1 expression		*p*-value
	High (n = 38)	Low (n = 37)	
Age (years)			
≥50	28	22	0.191
<50	10	15	
Gender			
Female	20	15	0.294
Male	18	22	
Tumor size (cm)			
≥5	24	14	0.028
<5	14	23	
TNM stage			
I-II	8	19	0.006
	30	18	
Differentiation			
Well-moderate	16	17	0.738
Poor	22	20	
Serum AFP			
Positive	26	24	0.744
Negative	12	13	
Vascular invasion			
Yes	22	11	0.014
No	16	26	
Cirrhosis			
Yes	27	20	0.128
No	11	17	

Alphafetoprotein: AFP.

2.3. Quantitative real-time PCR (qRT-PCR)

Total RNA was extracted by TRIzol reagent (Invitrogen) and cDNA was gained by PrimeScript RT Reagent Kit (TaKaRa, Dalian, China). Then, obtained cDNA was mixed with SYBR Green (TaKaRa) and specific primers (Table 2) to perform qRT-PCR. Besides, the nuclear and cytoplasm RNAs from HCC cells were extracted by PARIS Kit (Invitrogen). Fold change was analyzed by $2^{-\Delta\Delta Ct}$ method. All experiments were done in triplicate and repeated 3 times.

2.4. Colony formation assay

This assay is based on the principle that certain genes or proteins when expressed cause either cell cycle arrest or cell death, hence a reduction in colony number. In this, colony formation assay was used to measure cell survival fraction intensity (for evaluating radiosensitivity) and colony numbers (for assessing cell proliferation).

After transfection, HCC cells were seeded into 6-well plates and then exposed to the radiation (0, 2, 4 and 8 Gy) for 14 days. After fixed and stained, colonies were counted under a microscope (Olympus, Tokyo, Japan) to determine survival fraction intensity as the formula as previously described [16]: (number of irradiated colonies/number of cells plated)/(number of non-irradiated colonies/number of cells plated).

For assessing cell proliferation, the transfected and treated cells seeded into 6-well plates were cultured for 14 days. Colony numbers were counted under a microscope. All experiments were done in triplicate and repeated 3 times.

2.5. Cell counting kit 8 (CCK8) assay

The principle of CCK8 assay is as follows: the kit contains WST-8, which is oxidized and reduced by intracellular dehydrogenase to produce a water-soluble orange-yellow formazan that can be dissolved in culture medium, and the amount of formazan produced is proportional to the number of viable cells.

HCC cells were inoculated into 96-well plates and cultured overnight until cells attached to the plates. At the indicated time points, cells were cultured with CCK8 reagent for 2 h. Optical density (OD) value was assessed by a microplate reader (Thermo Labsystems, Waltham, MA, USA), and the relative OD ratio was used to express the cell proliferation capacity. The average value of 3 wells in each group was taken, and the experiment was repeated 3 times.

Table 2
Primer sequences used for qRT-PCR.

Name		Primers for qRT-PCR (5′−3′)
circROBO1	Forward	AGCTGGTGACATGGGTTCAT
	Reverse	TCACGTTCCCCAACCATATT
miR-136-5p	Forward	GTATGAACTCCATTTGTTTTGATGA
	Reverse	CAGTGCGTGTCGTGGAGT
RAD21	Forward	CACCGCCCACCAAGAAATTG
	Reverse	CCACAAAGGCTGAGCAGGTA
GAPDH	Forward	TCGGAGTCAACGGATTTGGT
	Reverse	TTCCCGTTCTCAGCCTTGAC
β-actin	Forward	CTTCGCGGGCGACGAT
	Reverse	CCACATAGGAATCCTTCTGACC
U6	Forward	ATTGGAACGATACAGAGAAGATT
	Reverse	GGAACGCTTCACGAATTTG

2.6. EdU assay

The principle of EdU assay is as follows: EdU is a thymidine analogue that can penetrate into the DNA molecules that are replicating in place of thymidine T during the period of cell proliferation, and the DNA replication activity of cells is rapidly detected based on the specific reaction of EdU with Apollo fluorescent dye.

The transfected and irradiated HCC cells were seeded in 96-well plates and stained with EdU solution following EdU Kit (Beyotime, Shanghai, China) instructions. Cells were imaged using a fluorescence microscope (Olympus) to count EdU positive cell rate using ImageJ software. The average value of 3 wells in each group was taken, and the experiment was repeated 3 times.

2.7. Flow cytometry

The principle of flow cytometry with Annexin V/PI double staining for apoptosis is as follows: at the beginning of early apoptosis, phosphatidylserine (PS) in the cell membrane flips from the inside to the outside of the lipid membrane. Annexin V labeled with FITC was used as a fluorescent probe to bind the everted PS, thereby detecting the occurrence of apoptosis. Propidium Iodide (PI) is a DNA-binding dye that can stain the nucleus of necrotic cells or cells that have lost their cell membrane integrity in the late stage of apoptosis.

HCC cells were collected and double-stained with Annexin V-FITC and PI (Beyotime). Cells were analyzed by flow cytometry (BD Biosciences, Franklin Lake, NJ, USA) and cell apoptosis rate was assessed by CellQuest software (BD Biosciences). The average value of 3 wells in each group was taken, and the experiment was repeated 3 times.

2.8. Western blot (WB) analysis

The basic principle of WB is to stain samples of cells or biological tissues that have been treated by gel electrophoresis by specific antibodies. By analyzing the location and depth of the staining, the expression of a particular protein in the cell or tissue under analysis is obtained.

Total protein was extracted by RIPA lysis buffer (Beyotime), separated with SDS-PAGE gel and transferred onto PVDF membranes. Membrane was treated with primary antibody against γH2AX (1:10000, ab81299, Abcam, Cambridge, MA, USA), cleaved-caspase3 (C-caspase3, 1:500, ab2302), RAD21 (1:5000, ab992), or β-actin

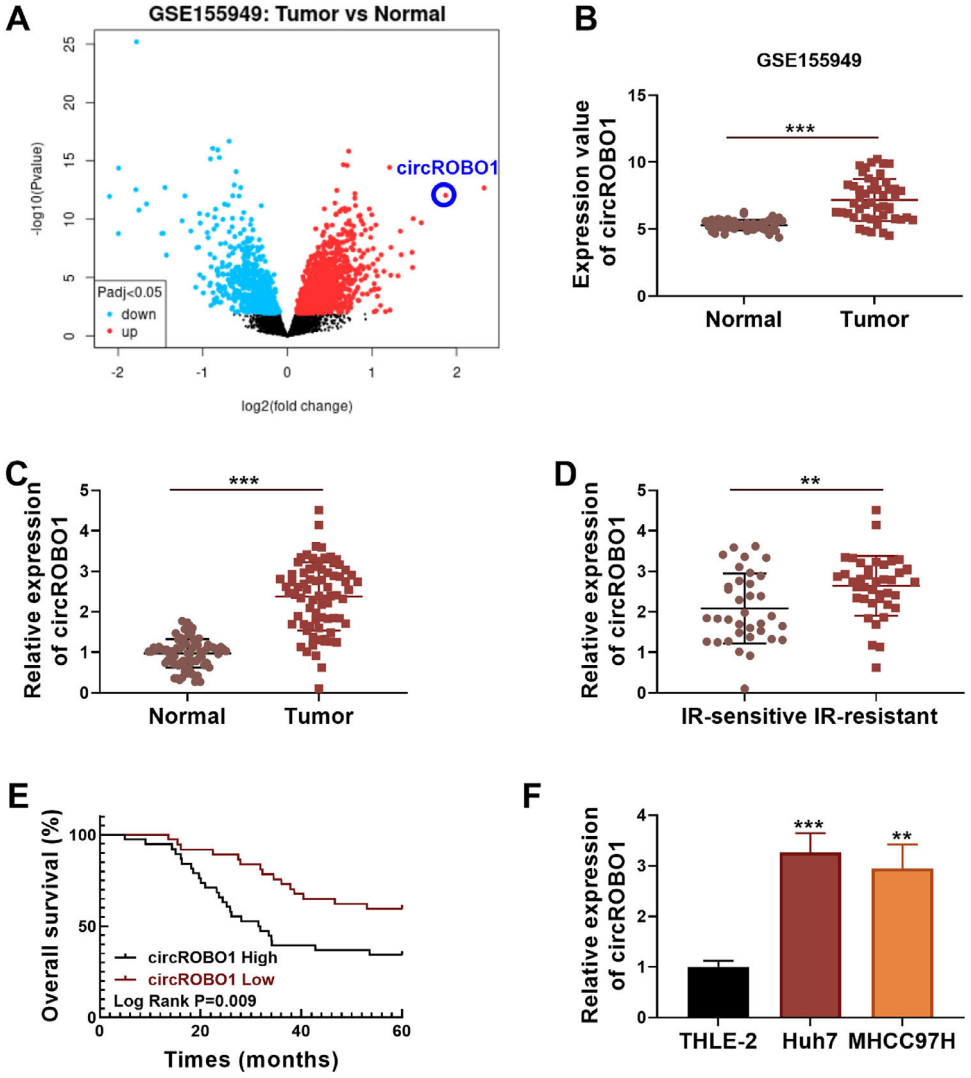

Fig. 1. CircROBO1 expression in HCC tissues and cells. (A) Volcanic map showed the differentially expressed circRNA in HCC tumor tissues and normal tissues analyzed by GEO database (GSE155949). (B) The expression value of circROBO1 in HCC tumor tissues and normal tissues analyzed by GEO database (GSE155949) was shown. (C) CircROBO1 expression was measured by qRT-PCR in HCC tumor tissues (n = 75) and adjacent normal tissues (n = 75). (D) CircROBO1 expression in the tumor tissues of IR-sensitive HCC patients (n = 35) and IR-resistant HCC patients (n = 40) was detected by qRT-PCR. (E) Kaplan-Meier analysis was used to analyze the correlation between circROBO1 expression and the overall survival of HCC patients. (F) CircROBO1 expression in HCC cells and THLE-2 cells was determined by qRT-PCR. $^{**}P < 0.01$, $^{***}P < 0.001$.

(1:1000, ab8227) followed by treated with secondary antibody (1:50,000, ab205718). Protein bands were detected by ECL reagents (Beyotime), and gray value was analyzed by ImageJ software. The average value of 3 wells in each group was taken, and the experiment was repeated 3 times.

2.9. Dual-luciferase reporter assay

According to the binding sites of miR-136-5p in circROBO1 or RAD21 3′UTR, we constructed the wild-type and mutant-type (circROBO1-WT/MUT or RAD21 3′UTR-WT/MUT) reporter vectors using pMIR-REPORT vectors. HCC cells were co−transfected with miR-136-5p mimic/miR-NC and vectors. Luciferase activity was determined by the Dual-Lucy Assay Kit (Solarbio, Beijing, China). The average value of 3 wells in each group was taken, and the experiment was repeated 3 times.

2.10. RNA pull-down assay

HCC cells were transfected with Bio-miR-136-5p-WT probe, Bio-miR-136-5p-MUT probe and Bio-miR-NC probe (Genepharma). The cell extracts were incubated with Dynabeads (Invitrogen). After

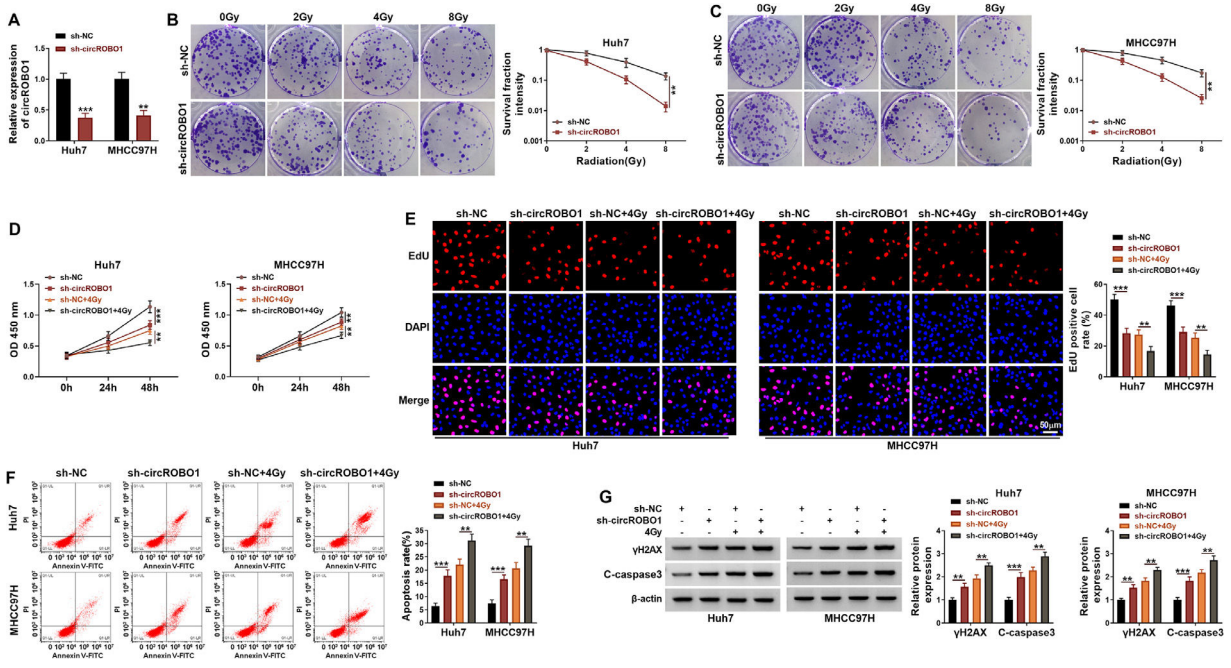

Fig. 2. Effects of sh-circROBO1 on the radiosensitivity of HCC cells. (A-C) Huh7 and MHCC97H cells were transfected with sh-NC or sh-circROBO1. (A) CircROBO1 expression was measured by qRT-PCR. (B-C) The radiosensitivity of HCC cells was analyzed by colony formation assay. (D-G) Huh7 and MHCC97H cells were transfected with sh-NC or sh-circROBO1 and treated with or without 4 Gy. CCK8 assay (D), EdU assay (E) and flow cytometry (F) were used to assess cell proliferation and apoptosis. (G) Protein expression was determined by WB analysis. $^{**}P < 0.01$, $^{***}P < 0.001$.

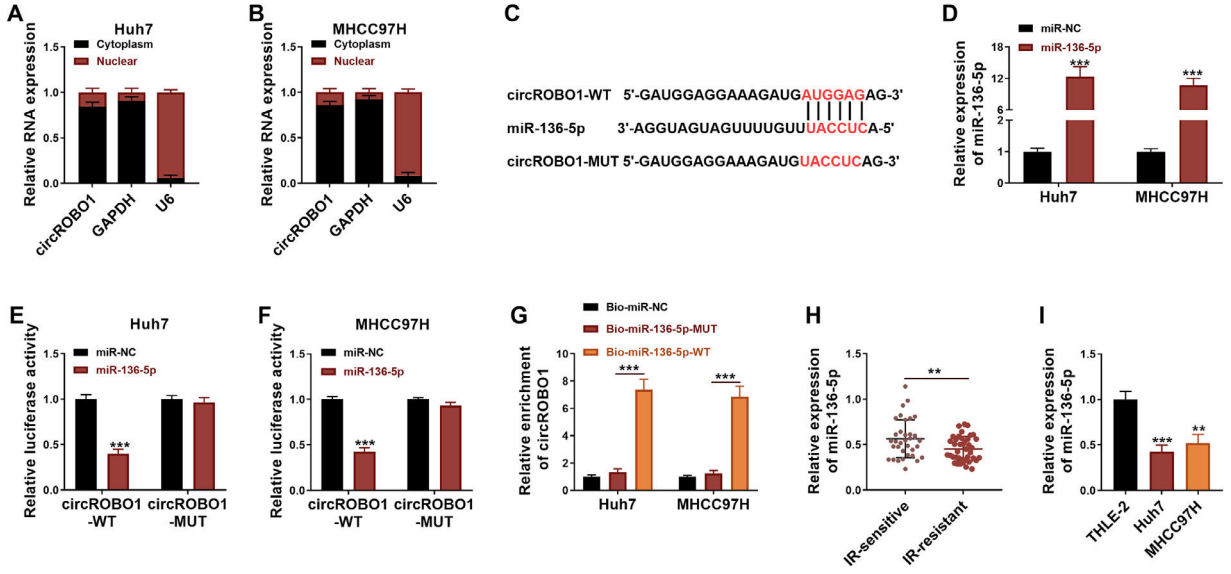

Fig. 3. CircROBO1 sponged miR-136−5p. (A-B) Subcellular localization analysis was used to analyze the distribution of circROBO1 in the cytoplasm and nuclear. (C) The sequences of circROBO1-WT/MUT were shown. (D) The transfection efficiency of miR-136−5p mimic was confirmed by qRT-PCR. Dual-luciferase reporter assay (E-F) and RNA pull-down assay (G) were performed to assess the interaction between them. (H) MiR-136−5p expression was detected by qRT-PCR in the tumor tissues of IR-sensitive HCC patients ($n = 35$) and IR-resistant HCC patients ($n = 40$). (I) MiR-136−5p expression was determined by qRT-PCR in HCC cells and THLE-2 cells. $^{**}P < 0.01$, $^{***}P < 0.001$.

extracted RNA, qRT-PCR was conducted to measure circROBO1 enrichment. The average value of 3 wells in each group was taken, and the experiment was repeated 3 times.

2.11. Animal experiments

Animal experiments were approved by the Animal Ethics Committee of Xiangyang Central Hospital, Affiliated Hospital of Hubei University of Arts and Science and were performed in compliance with the ARRIVE guidelines and the Basel Declaration. Male BALB/c mice (n = 20, Vital River, Beijing, China) were injected subcutaneously with Huh7 cells transfected with sh-NC/sh-circROBO1. When the tumor volume increased to 10 mm^3, mice were exposed with or without a single dose of 4 Gy radiation (n = 5/group) as previously described [17]. Tumor volume was measured every 7 days. 28 days later, tumor was removed for weighting and detecting protein expression. Also, the paraffin sections of tumor tissues were prepared to perform proliferation marker Ki67 immunohistochemistry (IHC) staining as previously described [17].

2.12. Statistical analysis

When evaluating results and analyzing data, personnel do not know in advance which group the data belong to. Results were expressed as mean ± SD. GraphPad Prism 7.0 software was used for date analysis. Differences were estimated using Student's t-test or ANOVA followed by Tukey post-hoc test. $P < 0.05$ was considered statistically significant.

2.13. Ethical statement

Written informed consent was obtained from each patient included in the study and the study protocol conforms to the ethical guidelines of the 1975 Declaration of Helsinki as reflected in a priori approval by the Ethics Committee of Xiangyang Central Hospital, Affiliated Hospital of Hubei University of Arts and Science.

3. Results

3.1. CircROBO1 was upregulated in HCC tissues and cells

The differentially expressed circRNA in 49 pairs of HCC tumor tissues and normal tissues were analyzed by GEO database (GSE155949), and circROBO1 was an overexpressed circRNA in HCC tumor tissues (Fig. 1A and B). In this, we detected circROBO1 expression in HCC tumor tissues and adjacent normal tissues using qRT-PCR and confirmed that it was significantly increased in HCC tumor tissues (Fig. 1C). Besides, we found that the expression of circROBO1 in the tumor tissues of IR-resistant HCC patients was higher than that in IR-sensitive HCC patients (Fig. 1D). According to the median of circROBO1 expression, HCC patients were divided into the circROBO1 high-expression group and the low-expression group. Through Kaplan-Meier analysis, it was found that the overall survival of patients in the circROBO1 high-expression group was significantly lower than that in the circROBO1 low-expression group (Fig. 1E). By analyzing the association between clinicopathologic features and circROBO1 expression in 75 patients with HCC, we found that high circROBO1 expression was associated with the tumor size, TNM stage, and vascular invasion of HCC patients (Table 1). In addition, the

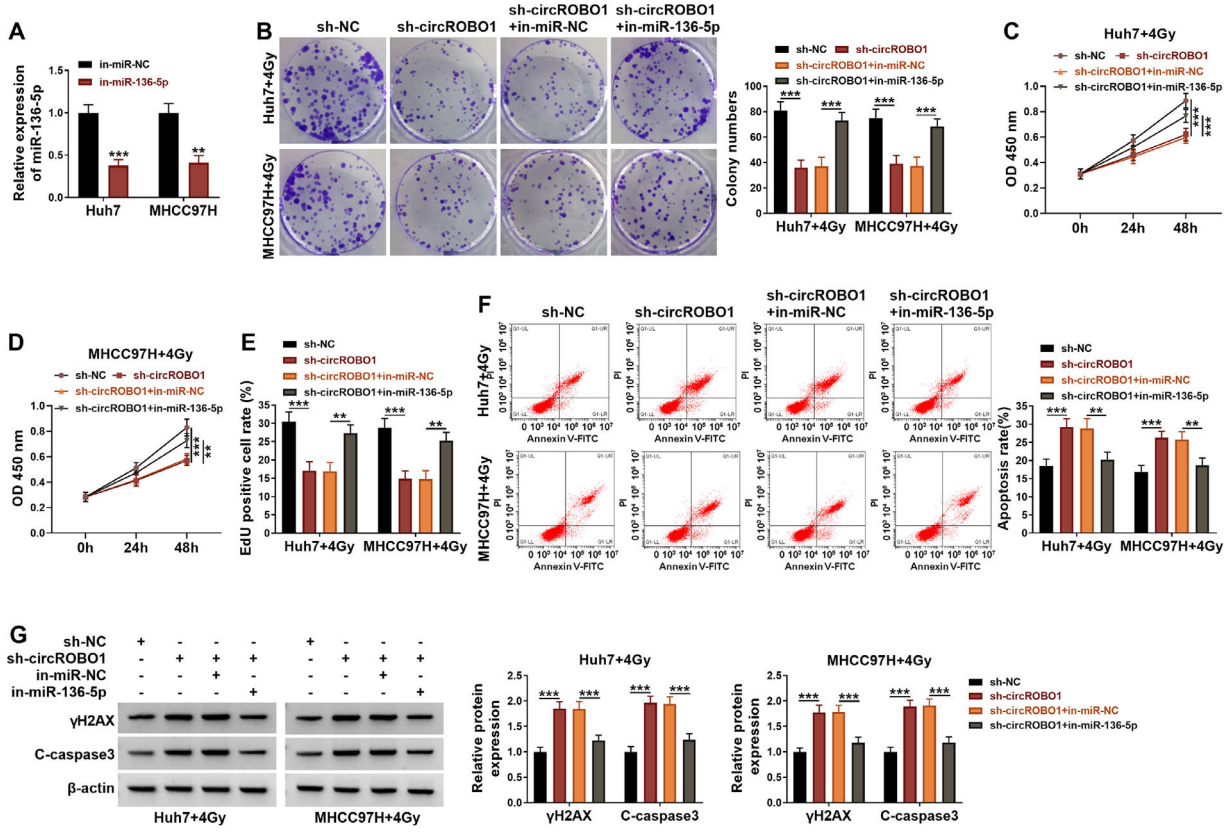

Fig. 4. Effects of sh-circROBO1 and in-miR-136-5p on the radioresistance of HCC. (A) The transfection efficiency of in-miR-136-5p was confirmed by qRT-PCR. (B-G) Huh7 and MHCC97H cells were transfected with sh-NC, sh-circROBO1, sh-circROBO1+in-miR-NC or sh-circROBO1+in-miR-136-5p, and then treated with 4 Gy. Colony formation assay (B), CCK8 assay (C-D), EdU assay (E) and flow cytometry (F) were performed to measured cell proliferation and apoptosis. (G) WB analysis was used to evaluate protein expression. $^{**}P < 0.01$, $^{***}P < 0.001$.

highly expressed circROBO1 also was confirmed in HCC cells (Huh7 and MHCC97H) compared with that in THLE-2 cells (Fig. 1F).

3.2. Downregulation of circROBO1 enhanced radiosensitivity in HCC cells in vitro

In order to verify the effect of circROBO1 in the radioresistance of HCC, Huh7 and MHCC97H cells were transfected with sh-circROBO1 to reduce circROBO1 expression in HCC cells (Fig. 2A). After inhibiting circROBO1, the survival fraction of cells was lower than that of the control group, suggesting that circROBO1 knockdown promoted the radiosensitivity of HCC cells (Fig. 2B and C). Silencing of circROBO1 suppressed cell viability and EdU positive cell rate, as well as aggravated the inhibition effect of radiation on cell viability and EdU positive cell rate (Fig. 2D and E). In addition, circROBO1 knockdown enhanced cell apoptosis rate, DNA damage marker γH2AX protein expression, and apoptosis marker C-caspase3 protein expression. Also, sh-circROBO1 elevated the promotion effect of radiation on cell apoptosis and the protein expression of γH2AX and C-caspase3 (Fig. 2F and G). These results revealed that knockdown of circROBO1 might alleviate the radioresistence of HCC.

3.3. CircROBO1 acted as a sponge of miR-136-5p

CircROBO1 was confirmed to be predominantly present in the cytoplasm (Fig. 3A and B), suggesting that circROBO1 had the potential to be a sponge of miRNA to mediate post-transcriptional regulation. The prediction results of circinteractome software (https://circinteractome.nia.nih.gov/index.html) showed that there had binding sites between circROBO1 and miR-136−5p (Fig. 3C). MiR-136−5p mimic was used to overexpress miR-136−5p in Huh7 and MHCC97H cells (Fig. 3D). In dual-luciferase reporter assay, the luciferase activity of circROBO1-WT vector was reduced by miR-136−5p mimic (Fig. 3E and F). Besides, circROBO1 enrichment was remarkably higher in the Bio-miR-136−5p-WT probe (Fig. 3G). These confirmed the interaction between circROBO1 and miR-136−5p. In addition, miR-136−5p was found to be lowly expressed in the tumor tissues of IR-resistant HCC patients and HCC cells (Fig. 3H and I).

3.4. Inhibition of miR-136-5p reversed the effect of sh-circROBO1 on the radioresistance of HCC in vitro

Then, in-miR-136-5p was used to reduce miR-136-5p expression in Huh7 and MHCC97H cells (Fig. 4A). The results showed that miR-136-5p inhibitor reversed the inhibitory effect of sh-circROBO1 on the colony numbers, viability and EdU positive cell rate of HCC cells under radiation treatment (Fig. 4B−E). Also, the positive regulation of sh-circROBO1 on the apoptosis rate and the protein expression of γH2AX and C-caspase3 under radiation treatment also were abolished by the addition of in-miR-136−5p (Fig. 4F and G). These data showed that circROBO1 regulated the radioresistence of HCC by mediating cell proliferation and apoptosis via sponging miR-136-5p.

3.5. miR-136-5p directly targeted RAD21

The StarBase software (http://starbase.sysu.edu.cn) predicted that miR-136-5p had binding sites in the 3′UTR of RAD21 (Fig. 5A). Further confirmation showed that miR-136-5p mimic only reduced the luciferase activity of RAD21 3′UTR-WT vector (Fig. 5B and C), verifying the interaction between miR-136-5p and RAD21. Besides, we

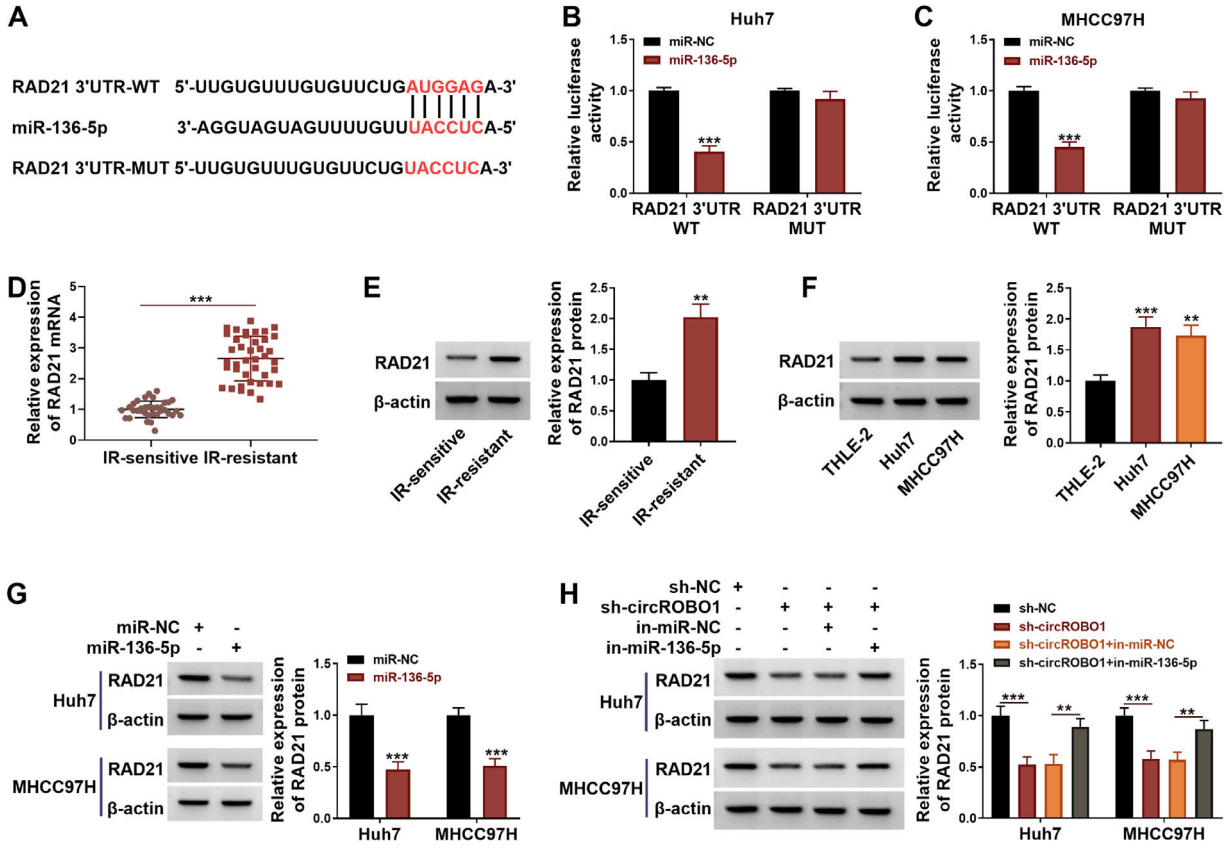

Fig. 5. MiR-136−5p targeted RAD21. (A) The sequences of RAD21 3′UTR-WT/MUT were shown. (B-C) Dual-luciferase reporter assay was performed to assess the interaction between them. (D-E) The mRNA and protein expression of RAD21 was analyzed by qRT-PCR and WB analysis in the tumor tissues of IR-sensitive HCC patients (n = 35) and IR-resistant HCC patients (n = 40). (F) RAD21 protein expression was measured by WB analysis in HCC cells and THLE-2 cells. (G) RAD21 protein expression was detected by WB analysis in HCC cells transfected with miR-NC or miR-136−5p. (H) WB analysis was used to examine RAD21 protein expression in HCC cells co-transfected with sh-circROBO1 and in-miR-136−5p. $^{**}P < 0.01$, $^{***}P < 0.001$.

observed that RAD21 mRNA and protein expression levels were significantly increased in the tumor tissues of IR-resistant HCC patients (Fig. 5D and E), and its protein expression also was higher in HCC cells than in THLE-2 cells (Fig. 5F). Overexpressed miR-136-5p had an inhibition effect on RAD21 protein expression (Fig. 5G). Also, circROBO1 knockdown markedly decreased RAD21 protein expression, and this effect was abolished by in-miR-136-5p (Fig. 5H). These results confirmed that circROBO1 sponged miR-136-5p to regulate RAD21.

3.6. RAD21 eliminated the regulation of sh-circROBO1 on the radioresistance of HCC in vitro

In order to further confirm that the regulation of circROBO1 on the radioresistance of HCC was achieved by mediating RAD21 expression, a rescue test was carried out. The pcDNA-RAD21 was used to increase RAD21 protein expression in Huh7 and MHCC97H cells (Fig. 6A). In functional experiments, sh-circROBO1-mediated the inhibition on the colony numbers, viability and EdU positive cell rate of HCC cells under radiation treatment could be reversed by RAD21 overexpression (Fig. 6B–E). The enhancing effect of sh-circROBO1 on the apoptosis rate and the protein expression of γH2AX and C-caspase3 under radiation treatment could be reversed by overexpression RAD21 (Fig. 6F–H). Above all, we confirmed that circROBO1 mediated the radioresistence of HCC through regulating RAD21.

3.7. Knockdown of circROBO1 enhanced the radiosensitivity of HCC tumors in vivo

In animal experiments, we found that circROBO1 knockdown reduced the tumor volume and weight of mice, and aggravated the sensitivity of radiation on mice tumor tissues (Fig. 7A and B). Through detecting the protein expression of γH2AX and C-caspase3, we observed that circROBO1 knockdown promoted DNA damage and cell apoptosis, and exacerbated the effect of radiation on the DNA damage and cell apoptosis in tumors (Fig. 7C). Also, Ki67 positive cells were reduced in sh-circROBO1 group and were also markedly decreased in sh-circROBO1+4 Gy group (Fig. 7D), confirming that downregulated circROBO1 aggravated the inhibition of 4 Gy on tumor cell proliferation.

4. Discussion

Radioresistance of tumor cells is a difficult problem in anticancer therapy. More and more studies have shown that circRNA can regulate miRNA/mRNA axis, thereby mediating the radioresistance process of cancers [18,19]. For example, circ-LARP1B had elevated expression in HCC tissues, and its knockdown reduced radioresistance of HCC cells via regulating miR-578/IGF1R axis [20]. This result indicates that circRNA may be a novel biomarker that can improve the radiosensitivity of HCC. Although Meng *et al.* elucidated the positive role of circROBO1 in the malignant progression of HCC [13], it remains unclear whether circROBO1 regulates radioresistance in HCC. Consistent with previous study [13], we confirmed the high circROBO1 expression in HCC patients. Further analysis showed that circROBO1 was markedly upregulated in IR-resistance HCC patients. According to our results, we found that circROBO1 knockdown improved HCC cell radiosensitivity, mainly by repressing cell proliferation and accelerating apoptosis. Moreover, down-regulation of circROBO1 could promote the radiosensitivity of tumors by reducing tumor cell proliferation and enhancing apoptosis. All data provided

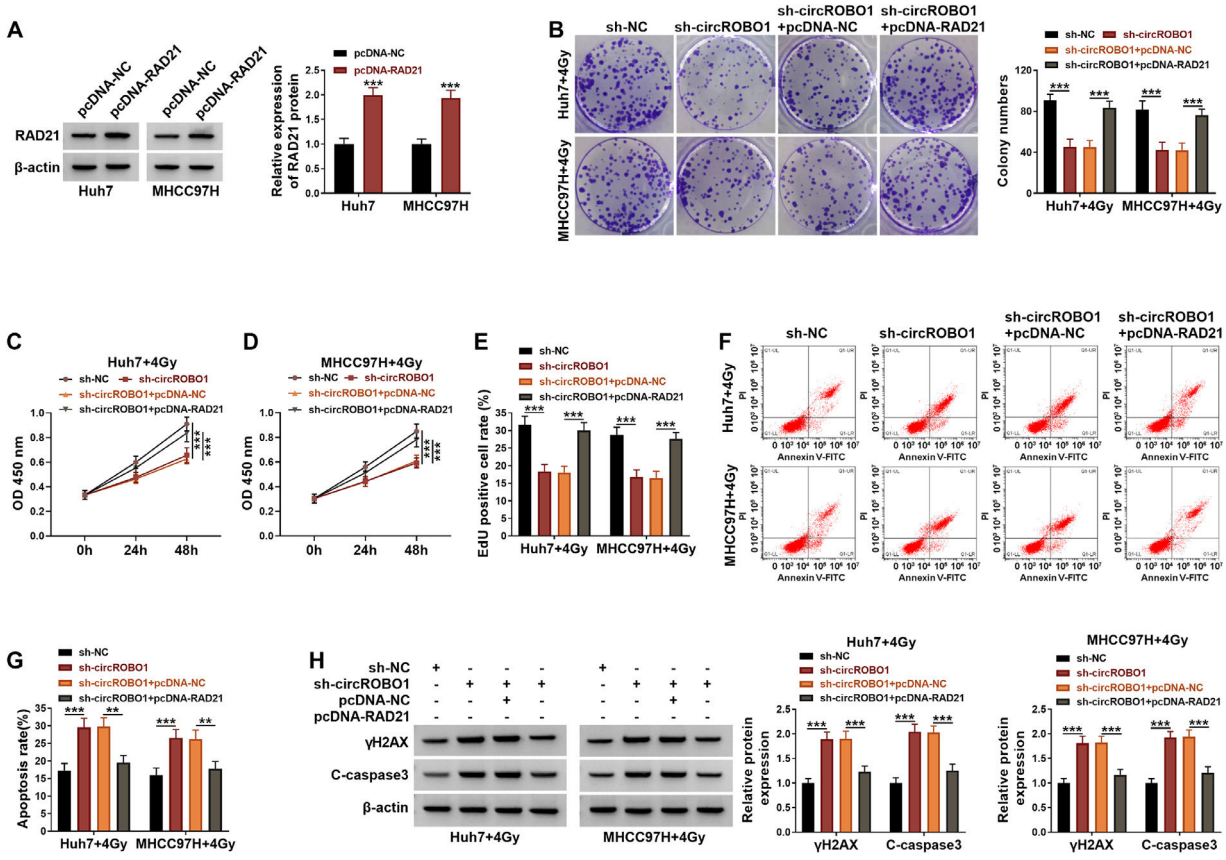

Fig. 6. Effects of sh-circROBO1 and RAD21 on the radioresistance of HCC. (A) The transfection efficiency of pcDNA-RAD21 was confirmed by WB analysis. (B-H) Huh7 and MHCC97H cells were transfected with sh-NC, sh-circROBO1, sh-circROBO1+pcDNA-NC or sh-circROBO1+pcDNA-RAD21, and then treated with 4 Gy. Cell proliferation and apoptosis were evaluated by colony formation assay (B), CCK8 assay (C-D), EdU assay (E) and flow cytometry (F-G). (H) WB analysis was utilized for examining protein expression. $^{**}P < 0.01$, $^{***}P < 0.001$.

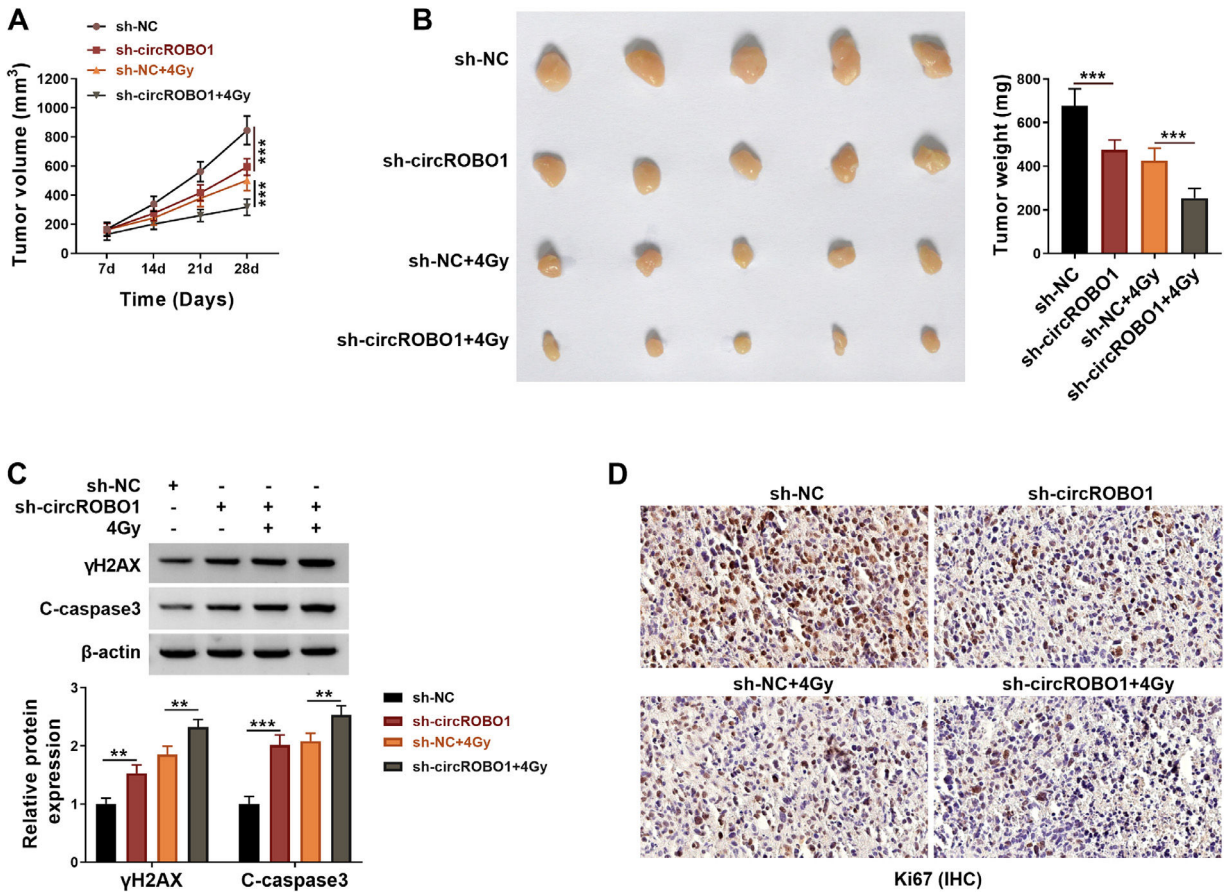

Fig. 7. Effects of sh-circROBO1 on the radiosensitivity of HCC tumors. Nude mice were injected with Huh7 cells transfected with sh-NC or sh-circROBO1, and then exposed with or without 4 Gy. Tumor volume (A) and weight (B) were measured. (C) Protein expression in tumor tissues was detected by WB analysis. (D) Ki67 positive cells were assessed by IHC staining. $^{**}P < 0.01$, $^{***}P < 0.001$.

evidence that circROBO1 was a potential therapeutic target for HCC radiosesistance, which was a new finding.

Based on the prediction results and further verification, we pointed out that circROBO1 acted as miR-136-5p sponge. Many researches had shown that miR-136-5p had an antitumor role in human cancers, including renal cell carcinoma [21] and breast cancer [22]. Previous study had reported that miR-136-5p promoted esophageal squamous cell carcinoma radiosensitivity by accelerating cell apoptosis [23]. In HCC, miR-136-5p was confirmed to be underexpressed and may be an anticancer miRNA that could inhibit cell proliferation and metastasis [24,25]. Here, we found that miR-136-5p was downregulated in IR-resistance of HCC patients, and its inhibitor also overturned sh-circROBO1-promoted radiosensitivity in HCC cells through increasing cell proliferation and decreasing apoptosis. These results verified that miR-136-5p improved the sensitivity of HCC cells to radiation, and circROBO1 indeed targeted miR-136-5p to mediate HCC radiosensitivity.

RAD21, a novel cohesin subunit, is involved in DNA fracture repair and meiosis recombination [26,27]. RAD21 has been found to be closely associated with cancer occurrence and patients' poor prognosis, including bladder cancer [28] and breast cancer [29]. Hepatitis C virus infection of hepatoma cells led to the upregulation of RAD21, which mediated the development of chronic hepatitis and HCC [30]. Past study suggested that RAD21 knockdown suppressed DNA damage repair to enhance the sensitivity of ovarian cancer cells to PARP inhibitors by inhibiting Akt/mTOR pathway [31]. Previous study revealed that RAD21 was overexpressed in tumor tissues and IR-insensitive HCC patients, and its overexpression reduced the 8-hydroxy-2-deoxyguanosine concentration and γH2AX level to attenuate IR treatment-induced DNA damage in HCC cells [32]. Consistent with the previous research, the high RAD21 level also was discovered in IR-resistance HCC patients. Through verification, we confirmed that circROBO1 sponged miR-136-5p to inhibit miR-136-5p function, thereby positively regulating RAD21. Functionally, our data presented that RAD21 overexpression revoked the regulation of sh-circROBO1 on the radiosensitivity of HCC, suggesting that RAD21 enhanced HCC radioresistence. Thus, we determined that circROBO1 regulated RAD21 through targeting miR-136-5p, thereby promoting the radioresistance of HCC.

Of course, there are some limitations of this study. CircRNAs are known to possess multiple mRNA binding sites. According to our conclusion, we pointed out that circROBO1 could enhance radioresistance of HCC by regulating miR-136-5p/RAD21 axis. Whether circROBO1 targets other miRNA/mRNA axes to regulate the radioresistance of HCC is still unclear. Of course, the more underlying mechanisms of the correlation between circROBO1 expression and IR resistance of HCC needs to be further explored in the further.

5. Conclusions

In conclusion, the present data indicated that circROBO1 regulated the miR-136-5p/RAD21 axis to promote the redioresistence of HCC. Our evidence showed that targeting the circROBO1/miR-136-5p/RAD21 axis might be an important measure to improve the radiotsensitivity of HCC.

Funding

This research did not receive any specific grant from funding agencies in the public, commercial, or not-for-profit sectors.

Declaration of interests

None.

Author Contributions

All authors have equally contributed to the conception, design, data collection, analysis, and writing of the manuscript.

References

[1] Hartke J, Johnson M, Ghabril M. The diagnosis and treatment of hepatocellular carcinoma. Semin Diagn Pathol 2017;34:153–9. https://doi.org/10.1053/j.semdp.2016.12.011.
[2] Clark T, Maximin S, Meier J, Pokharel S, Bhargava P. Hepatocellular carcinoma: review of epidemiology, screening, imaging diagnosis, response assessment, and treatment. Curr Probl Diagn Radiol 2015;44:479–86. https://doi.org/10.1067/j.cpradiol.2015.04.004.
[3] Zhang X, El-Serag HB, Thrift AP. Predictors of five-year survival among patients with hepatocellular carcinoma in the United States: an analysis of SEER-Medicare. Cancer Causes Control 2021;32:317–25. https://doi.org/10.1007/s10552-020-01386-x.
[4] Morris-Stiff G, Gomez D, de Liguori Carino N, Prasad KR. Surgical management of hepatocellular carcinoma: is the jury still out? Surg Oncol 2009;18:298–321. https://doi.org/10.1016/j.suronc.2008.08.003.
[5] Bamodu OA, Chang HL, Ong JR, Lee WH, Yeh CT, Tsai JT. Elevated PDK1 expression drives PI3K/AKT/MTOR signaling promotes radiation-resistant and dedifferentiated phenotype of hepatocellular carcinoma. Cells 2020:9. https://doi.org/10.3390/cells9030746.
[6] Wang J, Zhao H, Yu J, et al. MiR-92b targets p57kip2 to modulate the resistance of hepatocellular carcinoma (HCC) to ionizing radiation (IR) -based radiotherapy. Biomed Pharmacother 2019;110:646–55. https://doi.org/10.1016/j.biopha.2018.11.080.
[7] Zhang Z, Yang T, Xiao J. Circular RNAs: promising biomarkers for human diseases. EBioMedicine 2018;34:267–74. https://doi.org/10.1016/j.ebiom.2018.07.036.
[8] Han B, Chao J, Yao H. Circular RNA and its mechanisms in disease: from the bench to the clinic. Pharmacol Ther 2018;187:31–44. https://doi.org/10.1016/j.pharmthera.2018.01.010.
[9] Cui C, Yang J, Li X, Liu D, Fu L, Wang X. Functions and mechanisms of circular RNAs in cancer radiotherapy and chemotherapy resistance. Mol Cancer 2020;19:58. https://doi.org/10.1186/s12943-020-01180-y.
[10] Wang J, Chen Y, Wu R, Lin Y. Circular RNA hsa_circ_0000554 promotes progression and elevates radioresistance through the miR-485-5p/fermitin family members 1 axis in esophageal cancer. Anticancer Drugs 2021;32:405–16. https://doi.org/10.1097/CAD.0000000000001007.
[11] Zhao Y, Zhong R, Deng C, Zhou Z. Circle RNA circABCB10 modulates PFN2 to promote breast cancer progression, as well as aggravate radioresistance through facilitating glycolytic metabolism via miR-223-3p. Cancer Biother Radiopharm 2021;36:477–90. https://doi.org/10.1089/cbr.2019.3389.
[12] Yang W, Liu Y, Gao R, Xiu Z, Sun T. Knockdown of cZNF292 suppressed hypoxic human hepatoma SMMC7721 cell proliferation, vasculogenic mimicry, and radioresistance. Cell Signal 2019;60:122–35. https://doi.org/10.1016/j.cellsig.2019.04.011.
[13] Meng H, Li R, Xie Y, et al. Nanoparticles mediated circROBO1 silencing to inhibit hepatocellular carcinoma progression by modulating miR-130a-5p/CCNT2 axis. Int J Nanomedicine 2023;18:1677–93. https://doi.org/10.2147/IJN.S399318.
[14] Zhu L, Zhao Y, Yu L, et al. Overexpression of ADAM9 decreases radiosensitivity of hepatocellular carcinoma cell by activating autophagy. Bioengineered 2021;12:5516–28. https://doi.org/10.1080/21655979.2021.1965694.
[15] Wang B, Yang S, Zhao W. Long non-coding RNA NRAD1 and LINC00152 are highly expressed and associated with prognosis in patients with hepatocellular carcinoma. Onco Targets Ther 2020;13:10409–16. https://doi.org/10.2147/OTT.S251231.
[16] Jiang Y, Jin S, Tan S, Xue Y, Cao X. Long noncoding RNA NEAT1 regulates radiosensitivity via microRNA-27b-3p in gastric cancer. Cancer Cell Int 2020;20:581. https://doi.org/10.1186/s12935-020-01655-4.
[17] Jin Q, Hu H, Yan S, et al. lncRNA MIR22HG-derived miR-22-5p enhances the radiosensitivity of hepatocellular carcinoma by increasing histone acetylation through the inhibition of HDAC2 activity. Front Oncol 2021;11:572585. https://doi.org/10.3389/fonc.2021.572585.
[18] Liu J, Xue N, Guo Y, et al. CircRNA_100367 regulated the radiation sensitivity of esophageal squamous cell carcinomas through miR-217/Wnt3 pathway. Aging (Albany NY) 2019;11:12412–27. https://doi.org/10.18632/aging.102580.
[19] Du S, Zhang P, Ren W, Yang F, Du C. Circ-ZNF609 accelerates the radioresistance of prostate cancer cells by promoting the glycolytic metabolism through miR-501-3p/HK2 axis. Cancer Manag Res 2020;12:7487–99. https://doi.org/10.2147/CMAR.S257441.
[20] Zhu S, Chen Y, Ye H, et al. Circ-LARP1B knockdown restrains the tumorigenicity and enhances radiosensitivity by regulating miR-578/IGF1R axis in hepatocellular carcinoma. Ann Hepatol 2022;27:100678. https://doi.org/10.1016/j.aohep.2022.100678.
[21] Li J, Huang C, Zou Y, Ye J, Yu J, Gui Y. CircTLK1 promotes the proliferation and metastasis of renal cell carcinoma by sponging miR-136-5p. Mol Cancer 2020;19:103. https://doi.org/10.1186/s12943-020-01225-2.
[22] Han C, Fu Y, Zeng N, Yin J, Li Q. LncRNA FAM83H-AS1 promotes triple-negative breast cancer progression by regulating the miR-136-5p/metadherin axis. Aging 2020;12:3594–616. https://doi.org/10.18632/aging.102832.
[23] Huang HZ, Yin YF, Wan WJ, Xia D, Wang R, Shen XM. Up-regulation of microRNA-136 induces apoptosis and radiosensitivity of esophageal squamous cell carcinoma cells by inhibiting the expression of MUC1. Exp Mol Pathol 2019;110:104278. https://doi.org/10.1016/j.yexmp.2019.104278.
[24] Ding H, Ye ZH, Wen DY, et al. Downregulation of miR1365p in hepatocellular carcinoma and its clinicopathological significance. Mol Med Rep 2017;16:5393–405. https://doi.org/10.3892/mmr.2017.7275.
[25] Jia H, Wang H, Yao Y, Wang C, Li P. miR-136 inhibits malignant progression of hepatocellular carcinoma cells by targeting cyclooxygenase 2. Oncol Res 2018;26:967–76. https://doi.org/10.3727/096504018X15148192843443.
[26] Cheng H, Zhang N, Pati D. Cohesin subunit RAD21: from biology to disease. Gene 2020;758:144966. https://doi.org/10.1016/j.gene.2020.144966.
[27] Deardorff MA, Wilde JJ, Albrecht M, et al. RAD21 mutations cause a human cohesinopathy. Am J Hum Genet 2012;90:1014–27. https://doi.org/10.1016/j.ajhg.2012.04.019.
[28] Yu Z, Xu Q, Wang G, et al. DNA topoisomerase IIalpha and RAD21 cohesin complex component are predicted as potential therapeutic targets in bladder cancer. Oncol Lett 2019;18:518–28. https://doi.org/10.3892/ol.2019.10365.
[29] Yan M, Xu H, Waddell N, et al. Enhanced RAD21 cohesin expression confers poor prognosis in BRCA2 and BRCAX, but not BRCA1 familial breast cancers. Breast Cancer Res 2012;14:R69. https://doi.org/10.1186/bcr3176.
[30] Perez S, Gevor M, Davidovich A, et al. Dysregulation of the cohesin subunit RAD21 by Hepatitis C virus mediates host-virus interactions. Nucleic Acids Res 2019;47:2455–71. https://doi.org/10.1093/nar/gkz052.
[31] Gou R, Li X, Dong H, et al. RAD21 confers poor prognosis and affects ovarian cancer sensitivity to poly(ADP-Ribose)polymerase inhibitors through DNA damage repair. Front Oncol 2022;12:936550. https://doi.org/10.3389/fonc.2022.936550.
[32] Wang J, Zhao H, Yu J, et al. MiR-320b/RAD21 axis affects hepatocellular carcinoma radiosensitivity to ionizing radiation treatment through DNA damage repair signaling. Cancer Sci 2021;112:575–88. https://doi.org/10.1111/cas.14751.